Consequences of longer sealed curing on drying shrinkage, cracking and carbonation of concrete

Hamza Samouh, Emmanuel Rozière, Vincent Wisniewski, Ahmed Loukili

Consequences of longer sealed curing on drying shrinkage, cracking and carbonation of concrete

Hamza Samouh, Emmanuel Rozière, Vincent Wisniewski, Ahmed Loukili *

Institut de Recherche en Génie Civil et Mécanique (GeM), UMR-CNRS 6183, Centrale Nantes, France

The influence of sealed curing on long term drying behaviour and durability of concrete is investigated in this experimental study. Two concretes were cured for 16 h, 24 h, 48 h, and 1 month then exposed to drying at 20 °C and 50% RH. Mass loss, total and autogenous shrinkage were monitored. Hydration and microstructural development were studied by isothermal calorimetry and mercury intrusion porosimetry. The drying depth was assessed to quantify the heterogeneity of concrete specimens exposed to drying. The carbonated depth was measured after 6 months, 1 year and 4 years.

Longer sealed curing allowed better hydration of cement and reduced long term water loss. The curing duration significantly influenced the total and drying shrinkage magnitudes. Maximum values were found experimentally and numerically between 24 hour and 48 hour curing. The shrinkage induced cracking sensitivity was also affected; the shortest sealed curing duration resulted in the lowest cracking index.

Linear correlations were found between five properties: compressive strength and degree of hydration at exposure, carbonated depth, median pore diameter, and drying depth. These indicators can be used to optimize the durability of concrete. Sealed curing should be as long as possible to allow hydration of cementitious materials, to minimize drying depth, and to maximize the resistance to carbonation. However, drying shrinkage shows a pessimum; this should be taken into account in the design of durable concrete cover.

1. Introduction

The study of the influence of the initial conditions on the behaviour of cement based materials helps understanding the effect of the actual construction site conditions on the long term behaviour of concrete. After a longer curing period, concrete shows higher strength and stiffness due to better hydration of cement based materials [1 3]. A longer curing is also recommended to improve durability [4]. Long formwork duration allows a good hydration of cement, and thus reduces the free water content. At the same time, the capillary pores become finer and the water loss due to drying decreases [5 9]. Alhozaimy studied two moist curing periods (7 and 14 days), and concluded that the extended period led to a reduced concrete permeability especially in the presence of fly ash and at higher replacement levels [10]. The influence of curing time on these concrete properties involved in concrete durability is well known, but the published studies related to the influence of curing time on shrinkage are much scarcer.

Designing durable concrete cover actually requires taking into account shrinkage and cracking sensitivity, which was observed to increase with curing time in some published studies. As far as drying shrinkage is concerned, conflicting results have been reported in the literature. Miyazawa actually suggested that delayed sealed curing does not have a significant effect on drying shrinkage for concretes with three water cement ratios 0.4, 0.5, and 0.6 [11]. However, Aly and Sanjayan compared 1 day and 7 days curing, and confirmed that concretes cured for longer periods showed higher shrinkage [12]. Monge worked on a mortar exposed to drying after four curing durations 1 day, 2 days, 3 days and 7 days. He observed that shrinkage increased with curing time [6 7]. Mauroux confirmed this result on a mortar with and without cellulose for three periods: 1 day, 3 days and 7 days [8]. Hajibabaee monitored the curling of paste beams and simulated the development of effective pore pressure for three durations: no curing, 3 days, and 14 days to conclude that the developed internal pressure increased with the time of wet curing [13 15]. In order to assess shrinkage induced cracking, Monge conducted an experimental study and showed that cracks appear more rapidly with the long curing duration [6 7]. Most of these authors concentrated on capillary tension and the influence of pore sizes. As the pore radii decrease with curing time due to hydration, drying results in higher stresses thus higher shrinkage strain. These studies deal with specific conditions in terms of materials [6 8] or relatively short curing times, as the 28 day curing was not included. Only one published paper reported a pessimum initial curing time with respect to drying shrinkage [16]. In 1963, Perenchio

* Corresponding author.
E-mail address: ahmed.loukili@ec-nantes.fr (A. Loukili).

conducted a study published in 1997 where he stated that concrete pro duces the highest ultimate shrinkage between 3 and 7 days of curing, and lower shrinkage for 28 and 90 day curing. However the mecha nisms were not discussed in his paper.

This paper presents a comprehensive experimental study on the in fluence of sealed curing provided by formworks on shrinkage, micro structure, and durability of cement based materials. A new approach is described. It aims at understanding the effects of sealed curing dura tion on shrinkage and shrinkage induced cracking as well as other con crete properties involved in durability issues. The monitored properties are related to the hydration degree. The new notion of drying depth is used to analyse the drying shrinkage vs. mass loss curves and to inves tigate the impact of early drying on hydration and microstructure devel opment [17]. A simple model is used to confirm assumptions on the mechanisms involved in the observed pessimum curing time.

The RILEM Technical Committee 196 ICC classified the curing methods in two categories: external and internal curing as shown in Fig. 1. In this paper, demoulding is delayed to prevent the exchange of moisture with surrounding media. This method is within the scope of the external curing and, more specifically, the sealed curing definition given by Kovler and Jensen [17].

This paper aims to study the effect of the sealed curing duration on the long term behaviour of two types of concrete: vibrated concrete and self consolidating concrete. The experimental investigation in cludes the coupling between hydration and drying, long term shrink age, microstructure, and cracking sensitivity. Thus, hydration, drying and free shrinkage are monitored for the different curing durations. The microstructure is studied by mercury intrusion porosimetry (MIP). The carbonated depth is measured at different drying times and compared with drying depth, hydration degree at exposure and MIP results. The relation between drying depth which represents the skin effect (high porosity, high permeability, microcracking) and tradi tional concrete durability indicators (carbonated depth, median pore di ameter, degree of hydration and strength at exposure) are investigated. Finally, the risk of shrinkage induced cracking is estimated by the ring test.

2. Experimental procedures

2.1. Materials, mixtures, and curing

Ordinary Portland cement CEM I 52.5 N was used for both concrete mixes. Its chemical and physical properties are detailed in Table 1. Lime stone filler was used for self consolidating concrete mixture. Its calcium carbonate proportion was 97%, its density was 2.7 kg/m^3 and its Blaine surface 4350 cm^2/g. The coarse aggregates of sizes 10/14 and 6/10 mm were crushed amphibolite rocks with low water absorption (0.3%). The fine aggregate used in concrete was sea sand of granular class 0/4 mm. Its water absorption coefficient was 0.6%. A polycarboxylate based superplasticizer was used for SCC mixture.

As mentioned earlier, two concrete compositions were studied: self consolidating concrete (SCC) and vibrated concrete (VC) (Table 2). The water content W corresponds to the effective water content, i.e. the dif ference between total water content and water absorbed by aggregates.

Table 1
Cement oxide analysis, phase concentrations and Blaine fineness.

Oxide mass fractions (%)						
SiO_2	Al_2O_3	Fe_2O_3	CaO	MgO	SO_3	K_2O
19.6	4.5	2.3	63.7	3.9	2.6	0.7

Phase mass concentrations (%)					Physical properties	
Clinker	C_3S	C_2S	C_3A	C_4AF	Density (Kg/m^3)	Blaine (cm^2/g)
98	69	9	9	7	3.13	3900

Cylindrical specimens (7.8 cm in diameter and 28 cm in height) were made to study shrinkage, drying, and microstructure of SCC and VC. Both series of specimens were demoulded after different sealed cur ing periods at 20 °C constant temperature. Then they were stored in an air conditioned room at controlled temperature (20 ± 1 °C) and rela tive humidity (50 ± 5%). Three sets of SCC cylindrical specimens (Ø11 × 22 cm^2) of the same batch were demoulded after 16 h, 24 h, 48 h of sealed curing. Compressive strength and Young's modulus tests were performed on each set of specimens at ages of 16 h, 24 h, 48 h, 7 days, and 1 month (Table 3 and Table 4). The Young's modulus was determined by using LVDT sensors during compressive tests.

A second series of compressive tests were conducted on SCC and VC samples, immediately after demoulding. All specimens were kept in their moulds and stored in the climatic room at 20 °C constant temper ature until compressive testing time. According to these data (Table 3 and Table 4), the compressive strength and elastic modulus of SCC was not systematically higher than that of VC. SCC contains limestone filler which provides nucleation sites for the hydration products and in duces an acceleration of the hydration [18]. Consequently, the increase of strength and elastic modulus for SCC is higher at early age. However, the higher paste volume of SCC results in lower ultimate strength and Young's modulus [19]. The 28 day strength and elastic modulus of SCC were actually lower than VC.

The lowest sealed curing duration (16 h) lead to lower compressive strength during the first week. However, after one month the strength was not found to depend on the sealed curing duration, drying actually make menisci appear in the specimens exposed to drying before testing time. The effects of capillary tension were more significant for earlier demoulding because they had a longer time to develop and menisci fi nally reached finer pores. This provided concrete with higher apparent strength [20]. The observed tendency could also be partly due to the high water to cement ratio. In this studied case the earlier mould re moval slowed down the strength evolution without much affecting its long term value (Table 3). This slowdown can be explained by the cou pling between hydration and drying which mainly affects the external part of the specimen during the first days, but the relatively high avail able water content allowed hydration to go on slowly.

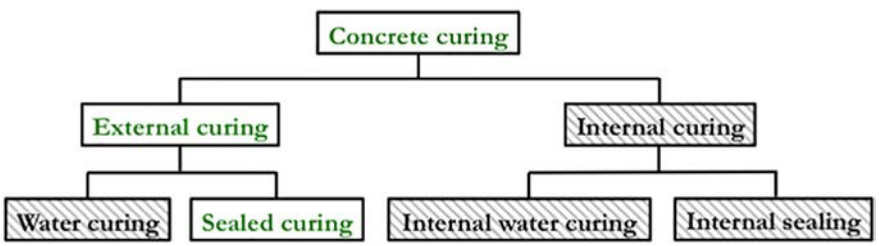

Fig. 1. Sealed curing and other curing means, adapted from [17].

Table 2
Concrete mixtures.

kg/m^3	SCC	VC
Gravel (amphibolite) 10/14 (G)	290	875
Gravel (amphibolite) 6/10 (G)	550	211
Sand 0/4 (S)	780	855
Cement (C)	330	303
Limestone filler (A)	210	–
Superplasticizer	2.8	–
Water (W)	205	182
V_G/V_S	0.92	1.1
W/C	0.62	0.60
W/(C + A)	0.38	0.60
Paste volume (L/m^3)	391	280

2.2. Degree of hydration

2.2.1. Heat of hydration

Cement hydration is an exothermal reaction and its rate is often assumed to be proportional to the heat flow to assess hydration degree. Isothermal calorimetry was used to measure this flow q for the SCC mixture. The TAM Air micro calorimeter was used. Its thermostat stability, limit of detection and precision are respectively ± 0.02 °C, 4 μW, and ± 20 μW. Two cylindrical glass bottles were used in this test. Their diameter was 6 cm and their height 7 cm. The first one was filled with 100 g of concrete; the second one which represents the reference sample was filled with the same mass and the same components except for cement replaced by an equal mass of sand. Since the heat capacity of sand and cement were assumed equal, this method provides us with an inert reference while keeping an equivalent heat capacity.

At a given time, the degree of hydration $\alpha(t)$ can be approximated as the ratio of the cumulated heat $Q(t)$ and the cumulated heat at complete hydration Q_{tot} [21] (Eq. (1)).

$$\alpha(t) \approx \xi(t) \quad \frac{Q(t)}{Q_{tot}} \quad \frac{\int_0^t q(\tau)d\tau}{Q_{tot}} \tag{1}$$

The heat flow was measured for 6 weeks. Root square equation was used to obtain the heat at complete hydration. Graphically, plotting cumulated heat flow vs. $1/t^{0.5}$ gives a straight line near zero. Its intersection with the y axis gives an estimation of the cumulated heat at complete hydration. A previous study with the same device showed that the difference between two samples is generally lower than 2% [22].

2.2.2. Chemically and physically bound water

After drying at (20 °C, 50% RH), three specimens (Ø7.8 × 28 cm^2) initially protected during three sealed curing durations (16 h, 24 h, 48 h) were stored in the oven at 105 °C until stabilization of mass (mass change not exceeding 0.05% after 24 h [23]). The mass loss evolution during the first four years was extrapolated to obtain the ultimate mass loss under (20 °C, 50% RH). The mass loss in the oven was also measured. The sum of these two values was assumed to give the evaporable water content of concrete [24].

Then three samples (Ø7.8 × 1.5 cm^2) were sawn from each specimen and they were dried in the oven in the same conditions during one week until stabilization. Finally, they were stored in another oven under 600 °C during approximately 24 h until stabilization of mass in order to assess chemically bound water. This amount is generally determined by heating specimens from 105 °C to 1000 °C and measuring the mass loss. Thermogravimetric (TG) analyses have shown that the main mass loss between 600 and 1000 °C corresponds to $CaCO_3$ decarbonation. A peak can actually be observed on DTG curve between 600 °C and 750 °C [25]. The mass loss at 600 °C was measured and this value was used to assess the chemically bound water.

2.3. Free shrinkage and mass loss

The experimental procedure to measure the time dependent strains was based on the recommendations of the RILEM Technical report [26]. The cylindrical specimens (Ø7.8 × 28 cm^2) were moved immediately after casting to an air conditioned room at 20 ± 1 °C and 50% RH. The specimens were demoulded after sealed curing periods presented in Table 5. The top and bottom surfaces of total shrinkage and mass loss specimens were covered with an adhesive backed aluminium foil, to achieve two dimensional drying (Fig. 2). The total shrinkage and mass loss were measured on these specimens immediately after removing the moulds (within 3 min). LVDT sensors were used to monitor the shrinkage strains (one hour interval). The specimens used to measure autogenous shrinkage were carefully protected against drying from the start of testing. Six months later, only an average of 0.03% mass loss was observed on the sealed specimens [27]. The use of a double layer of adhesive backed aluminium foil is actually more effective than acrylic, latex, or epoxy protection [28]. The drying shrinkage was deduced as the difference between the measured total shrinkage and autogenous shrinkage [29].

The total shrinkage strain at a given time cannot be considered as an intrinsic parameter of the material. The shrinkage magnitude actually depends on the measurement duration, and the classification can be reversed with time [30 31]. Several models can be used to analyse drying shrinkage curves through two parameters: characteristic time and ultimate drying shrinkage. The hyperbolic equation is the most common form today [32 33]. Eq. (2) used in this study was first introduced by Hansen et al. [34]. t_0 is the duration of sealed curing.

$$\varepsilon_{dry} \quad \frac{(t-t_0)}{(t-t_0)+N_s}\varepsilon_\infty \tag{2}$$

Both parameters, ultimate shrinkage ε_∞ and shrinkage half time N_s, were determined from the experimental data so as to minimize the mean square error. Fig. 3 represents the calibration of the parameters on SCC, for $t_0 = 48$ h. The repeatability of the approach was estimated on SCC by analysing two data series for three sealed curing durations. The ultimate drying water $W_{dry}(\infty)$ was deduced by the same mathematical form from experimental mass loss evolution as shown in Fig. 4.

Table 3
Strength for different sealed curing durations.

	Test time Sealed curing duration	16 h f_c MPa	24 h f_c MPa	48 h f_c MPa	7 days f_c MPa	1 month f_c MPa
SCC	16 h	9.7 ± 1.0	12.2 ± 1.3	20.5 ± 1.6	28.9 ± 2.2	34.5 ± 3.1
	24 h	–	16 ± 0.1	23.2 ± 0.6	31.3 ± 0.3	35.7 ± 0.0
	48 h	–	–	21.5 ± 0.4	32.3 ± 0.6	34.5 ± 3.1
	Until testing	10 ± 0.0	17.4 ± 0.0	24.4 ± 0.1	x	35.4 ± 0.1
VC	Until testing	6.0 ± 0.1	13.1 ± 0.2	21.0 ± 0.6	x	38.0 ± 1.0

Table 4
Young's modulus for different sealed curing durations.

	Test time Sealed curing duration	16 h E GPa	24 h E GPa	48 h E GPa	7 days E GPa	1 month E GPa
SCC	16 h	18.2 ± 2.2	20.5 ± 2.7	29.0 ± 3.2	34.1 ± 4.8	x
	24 h	–	21.8 ± 1.2	28.8 ± 0.4	33.7 ± 1.5	x
	48 h	–	–	29.3 ± 0.6	37.9 ± 1.3	x
	Until testing	12.8 ± 1.4	22.0 ± 1.5	24.7 ± 1.6	x	31.4 ± 1.6
VC	Until testing	12.1 ± 0.5	19.5 ± 0.2	26.4 ± 1.0	x	33.6 ± 0.2

2.4. Mercury intrusion porosimetry

Mercury intrusion porosimetry measurements were performed with Micromeritics Autopore IV 9500 porosimeter. 1.5 cm^3 cubic samples of the material were sawn from the centre and the edge of the cylindrical SCC specimens (Fig. 5) exposed to drying for 6 months after different periods of sealed curing. The notion of median pore diameter was used to interpret results. It is defined as the pore diameter at which 50% of the total intruded volume of mercury is intruded into the sample [35]. Previous study shows that the uncertainty on the total porosity was ±2.5% of the average value [22].

2.5. Carbonation

Carbonation is the most common environmental actions. Corrosion of steel reinforcement is likely to occur when the concrete cover has been carbonated. In this study the progress of the carbonation front was studied on cylindrical specimens exposed to drying at 20 °C and 50% RH. Carbonated depth was assessed by a colorimetric method based on phenolphthalein used as an indicator in acid base titrations [36 37]. It turns colourless in carbonated concrete and pink in basic area. The phenolphthalein solution was sprayed on cross sections of cylindrical specimens of SCC (Fig. 5). For each specimen, five measurements of carbonated depth were operated and the average value was considered. The test was performed after three drying times: 6 months, 1 year and 4 years.

2.6. Restrained shrinkage

The ring test was used to estimate the cracking sensitivity of concrete. According to ASTM approach [38], the steel ring strain and the cracking time are used to calculate two indicators, which classify the potential for cracking into four categories: low, moderate low, moderate high and high. Kovler merged these two indicators in one parameter named integrated criterion [39,40]. However, the circumferential drying described by ASTM and AASHTO [38,41] gives a complicated stress distribution which changes shape over time [42]. In the experimental study presented in this paper the lateral protection from drying was chosen, as it provides a uniform shrinkage along the radial direction and defined shape of residual stress [37]. Steel rings have been developed at GeM Laboratory in order to investigate restrained shrinkage. Their geometry and dimensions were chosen to reproduce the restraint conditions of structural walls [43]. The ring test can used to measure restrained shrinkage strains and to estimate the cracking sensitivity of the concrete. The dimensions of the ring are: a = 8.5 cm; b = 11 cm; c = 18 cm, where a is the inner radius of the inner steel ring, b is the outer radius of the steel ring, and c is the outer radius of the concrete ring (Fig. 6). The thickness of the concrete ring was equal to 5 times the maximum aggregate size (7 cm = 5 × 1.4 cm).

Based on Kovler studies, integrated criterion i_{cr} can be defined as the ratio between both criteria (Eq. (3)): S (average stress rate) and t_{cr} (elapsed time at cracking or elapsed time at the end of the test (day)) [39]:

$$i_{cr} \quad \frac{S}{t_{cr}} \tag{3}$$

The stress rate in each test specimen at cracking or end time is determined by Eq. (4):

$$q \quad \frac{G\alpha}{2\sqrt{t_{cr}}} \tag{4}$$

q: stress rate in each specimen (MPa/day),
G: ASTM value was 72.2 GPa; the configuration and geometry of our ring give G = 185 MPa [27,44],
α: the average strain rate factor for each specimen (m/m)/$day^{1/2}$.

The dimensions and drying sides of the ring used in the experimental study differs from ASTM rings, thus the assessment of the cracking

Table 5
Experimental program.

Concrete mixture	Test	Sealed curing			
		16 h	24 h	48 h	1 month
SCC	Mass loss	✓	✓	✓	✓
	Shrinkage	✓	✓	✓	✓
	Ring test	✓	✓	✓	
VC	Mass loss	✓		✓	
	Shrinkage	✓	✓	✓	
	Ring test		✓		

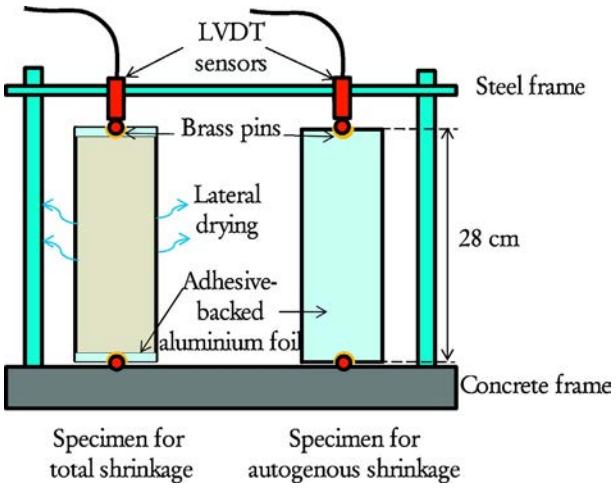

Fig. 2. Test rig used for the measurement of total and autogenous shrinkage.

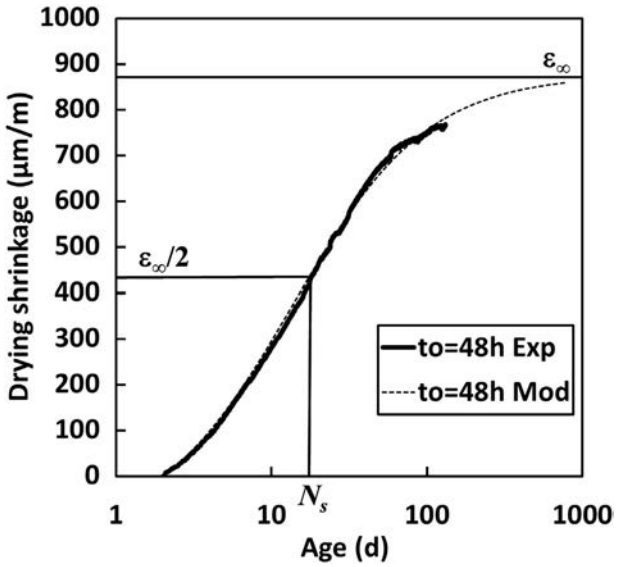

Fig. 3. Drying shrinkage vs. age after 48 h sealed curing duration for SCC: experimental and model curves.

sensitivity requires adapted intervals of the potential of cracking. In a previous study [27,45], three intervals have been defined:

Low risk for: $i_{cr} \leq 1$
Medium risk for: $1 \leq i_{cr} \leq 3$
High risk for: $i_{cr} \geq 3$.

3. Experimental results and discussion

3.1. Drying and free shrinkage

3.1.1. Drying and hydration

Table 6 gives the evolution of the degree of hydration estimated by the measurement of the heat flow for SCC. The real progress of the hydration degree is given at the time of exposure. It doubled between 16 h and 48 h than tripled between 16 h and 1 month. The corresponding chemically bound water W_{hyd} was deduced by Eq. (5). The longer the sealed curing duration is the lower free water content becomes. Thus, the coupling of hydration and drying becomes weaker for a long curing period.

$$W_{hyd}(t) \quad \alpha(t) W_\infty C \tag{5}$$

where $\alpha(t)$ is the evolution of hydration degree, determined by isothermal calorimetric analysis, W_∞ is the ultimate value of the chemically bound water to cement content ratio (Kg/Kg), the 0.25 value resulted from the composition of the cement given in Table 1 taking into account the volume of water required for the hydration of each phase [21,46 48], and C is the cement content given by Table 2 (Kg/m^3).

Linear [46] or parabolic [49] formulae can be used to describe the relation between the compressive strength and the degree of hydration. De Schutter et al. gave a general formulation for this relation [50]. However, as shown in Fig. 7, the linear equation perfectly fitted the experimental data. The four points give the values corresponding to the four sealed curing durations.

The classification of mass loss curves observed in Figs. 8 and 9 was expectable, since the specimens demoulded after a shorter period of time were exposed to drying before complete hydration of cement thus lose a higher amount of capillary water [5,51]. In the drying conditions of the study, the free water was released in an irreversible manner. At long term a gap remains between the ultimate mass losses associated to the different sealed curing durations (Fig. 8 and Fig. 9). This difference can be associated with the bound water, whether it is linked chemically (solid gel) or physically (in gel pores). A delayed curing actually allows a better hydration of cement, and increases the amount of chemically bound water before exposure to drying, especially for concrete with low water to cementitious materials ratio. Moreover, in regards to the physically bound water (adsorbed at surfaces of gel particles), the progress of the hydration results in an increase in the specific surface of solid gel thus higher adsorbed water to free water ratio. The porous network becomes finer and the hydric gradient requested to evaporate the same amount of water becomes higher. Thus, a delayed curing period induces an increase in physically bound water and free water content at equilibrium at a given relative humidity [47].

Fig. 10 shows the evolution of the volumetric phase distribution of the water in the concrete specimens exposed to drying. The water content in the specimen varies locally due to hydric gradients, thus the graph only gives global distributions. The diagram starts at the contact of water with cement and finishes with the end of hydration. Three phases are presented: drying water, chemically bound water, and finally free and gel water (capillary and physically bound water [52]). The evolution of the first phase began when the specimens were demoulded. Its ultimate value decreased with the sealed curing duration, as it was shown by the curves of mass loss (Figs. 8 and 9). After drying at 20 °C and 50% RH, the specimens were stored at 105 °C and 2% RH until stabilization of mass. The evaporable water under these conditions can be deduced and plotted (Fig. 10).

The chemically bound water until t_0 was calculated by Eq. (5). The maximum degree of hydration ($\alpha = \alpha_{max}$) corresponding to ($t \rightarrow \infty$) for each sealed curing duration was calculated from the same equation by using the measured mass loss at 600 °C. The values were lower than the ultimate hydrated water deduced for ($\alpha = 1$).

Finally, the sum of capillary water W_{cap} and gel water W_{gel} was approximated as the difference between the initial water and the sum of chemically bound water and drying water as shown in Eq. (6).

$$W_{cap}(t) + W_{gel}(t) \quad W - W_{hyd}(t) - W_{dry}(t) \tag{6}$$

The ultimate degree of hydration was higher for the shortest sealed curing ($t_0 = 16$ h), although the water lost by evaporation was greater in this case. Xi, Bazant and Jennings actually showed that a higher degree of saturation is reached for a given relative humidity when exposure to drying start is delayed [53]. Thus the water amount available

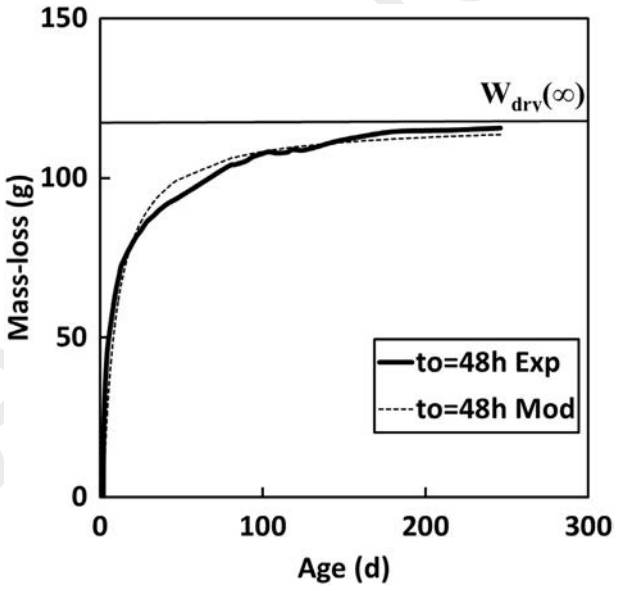

Fig. 4. Mass-loss vs. age after 48 h sealed curing duration for SCC: experimental and model curves.

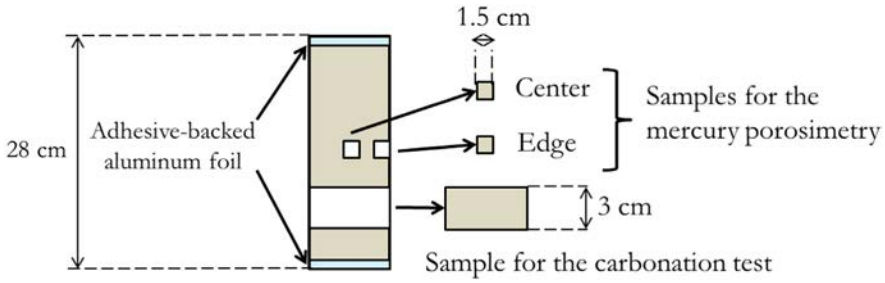

Fig. 5. Samples for mercury intrusion porosimetry and carbonation tests.

for hydration is theoretically higher for the longest sealed curing periods. However, the progress of hydration cannot be considered as stopped by drying at such high W/C ratio. The observed tendency could be explained by an increase in the gel water with curing. For instance, when α reached 0.8 the sum of capillary and gel water was approximately the same for the three sealed curing durations, but for the longest curing period a larger proportion of this water was physically bound. More water was actually adsorbed at surfaces of cement gel particles, and the water available for hydration was lower. Thus the hydration continued for the specimen with short sealed curing duration and reached higher levels, despite that the water evaporated during the first stage (at 20 °C, 50% RH) was greater.

3.1.2. Shrinkage

The shrinkage measurements have been conducted twice on the same SCC mixture, and once on the vibrated concrete to get more reliable results. The SCC showed higher autogenous and total shrinkage than VC (Fig. 11 and Fig. 12). After one month the autogenous shrinkage has generally reached >80% of the final value [54]. Autogenous shrinkage is actually caused by hydration and self desiccation shrinkage. After one month of sealed curing a relatively high hydration degree is reached (Fig. 10), thus autogenous shrinkage cannot significantly develop from this time. The autogenous shrinkage magnitude can be considered lower for SCC (100 μm/m) compared to the VC (75 μm/m). The ultimate drying shrinkage of SCC and VC were assessed from experimental data and model (see Section 2.3). They are given in Table 6. In all cases SCC showed higher ultimate drying shrinkage and shrinkage halftime. The drying shrinkage magnitude is actually known to increase with paste volume [51,55]. The lower shrinkage rate of SCC could be due to lower permeability [56], which delays the equilibrium between internal and ambient relative humidities. Both concrete mixtures had approximately the same W/C ratio (Table 2), but the W/(C + A) of SCC was much lower.

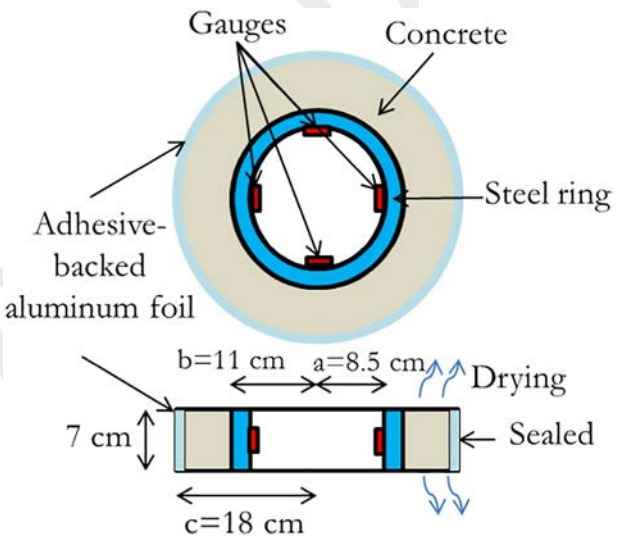

Fig. 6. Experimental disposition of the ring test.

Whatever the data series, the long term drying shrinkage was higher for specimens demoulded after a longer time, up to 48 h sealed curing duration. The same classification was obtained for total and drying shrinkage. The model given by Eq. (2) can be used to analyse the drying shrinkage results. The ultimate shrinkage and shrinkage half time for different initial conditions are presented in Table 7. The ultimate shrinkage for $t_0 = 48$ h was slightly higher than at $t_0 = 24$ h, and that of $t_0 = 16$ h was significantly lower. From $t_0 = 48$ h to $t_0 =$ 1 month, the shrinkage magnitude decreased, but remained higher than that obtained for $t_0 = 16$ h. This suggests the existence of a pessimum curing duration after 48 h as proposed by Perenchio [16]. Shrinkage half time did not significantly vary for SCC. Nevertheless, for VC a low value was observed for $t_0 = 48$ h, which corresponds to a three times faster drying shrinkage.

Even if these results are consistent with previous studies [8,13,14,15,57], they can be surprising at first glance. It is actually recommended to keep the formworks and extend sealed curing as long as possible to get better strength and durability. However, the influence of sealed curing duration on shrinkage magnitude is not taken into account in code models such as Eurocode 2 [27], CEB [58], ACI [59], and B4 [60].

In order to understand better why lower mass loss lead to higher drying shrinkage the drying shrinkage vs. mass loss curves were plotted for SCC in Fig. 13 and VC in Fig. 14. Two stages can be observed. Shrinkage tests did not last long enough to observe the third stabilization stage [30]. The first stage of the curves, which corresponds to the mass loss without inducing drying shrinkage, was shorter for specimens that were kept for a longer time in formworks. For a sufficiently delayed formwork removal and a more mature material, this first stage seems to disappear. This observation will be discussed in the following Section (3.1.3 Drying depth).

3.1.3. Drying depth

The first stage of the shrinkage vs. mass loss graphs corresponds to the external layer of concrete, which quickly loses free water until equilibrium [17]. The drying depth depends on the concrete mixture, the initial or external conditions. It includes several phenomena that can lead

Table 6
Hydration and drying: chemically bound water content W_{hyd} and mass-loss W_{dry} of SCC specimens exposed to drying after sealed curing.

Age	16 h	24 h	48 h	1 month
α(%)	30	45	63	91
$W_{hyd}(t_0)$ (g)	33.1	49.6	69.5	100.4
$W_{dry}(\infty)$ (g)	134	129	118	99
$W_{hyd}(t_0)/W$ (%)	12.1	18.1	25.4	36.6
$W_{dry}(\infty)/W$ (%)	48.9	47.1	42.3	39.0

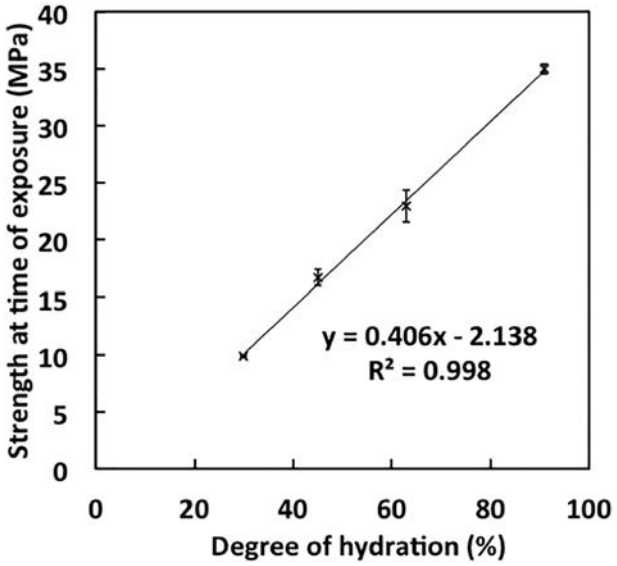

Fig. 7. Strength at time of exposure vs. degree of hydration for the SCC.

to the observed drying shrinkage behaviour, namely: coupling between hydration and drying [61], micro cracks [62 63] and wall effect due to formwork [64 65]. However, these phenomena cannot be easily distinguished.

The "drying depth" can directly be deduced from the shrinkage vs. mass loss curves [30,66], by converting the mass loss into an equivalent distance. This can be estimated by dividing the mass loss to drying surface ratio by the initial free water content of concrete, which depends on the concrete mixture. This ratio is noted as d (Eq. (7)). The drying depth δ is defined as the intersection between the linear extrapolation of the second stage and the horizontal axis in the drying shrinkage versus d curve, as shown in Fig. 15 and Fig. 16.

$$d \quad \frac{m(t)-m(t_0)}{m_f * S_d} \tag{7}$$

$(m(t) - m(t_0))$: mass loss of specimen (Kg)

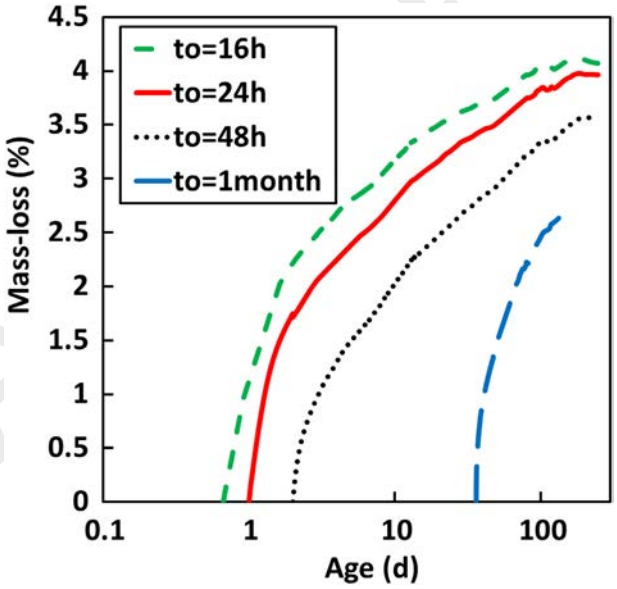

Fig. 8. Mass-loss vs. age for SCC.

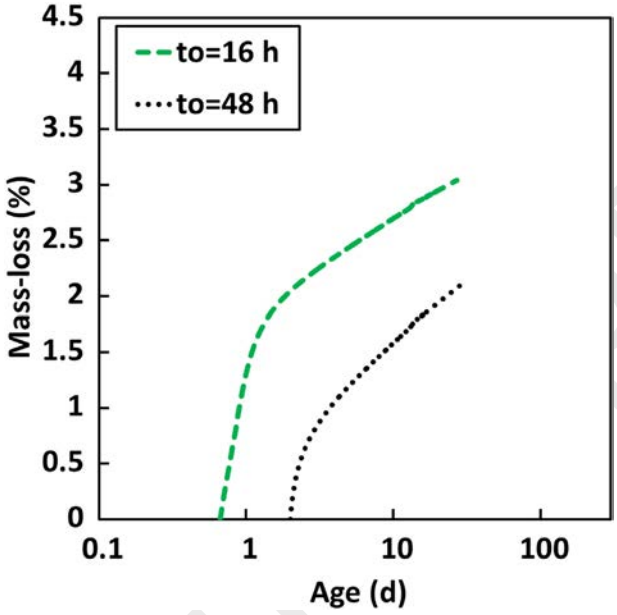

Fig. 9. Mass-loss vs. age for VC.

S_d: drying surface of specimen (m^2)

m_f: free water mass in 1 m^3 of concrete at t_0 given by Eq.uation (8) (Kg/m^3).

$$m_f \quad W-W_{hyd}(t_0) \quad W-\alpha(t_0) * W_\infty * C \tag{8}$$

W is the effective water content given in Table 2 (Kg/m^3).

$\alpha(t_0)$ is the hydration degree when concrete is exposed to drying, estimated by isothermal calorimetric analysis for SCC. Fig. 7 showed a linear relation between the degree of hydration and compressive strength at time of exposure. Thus the degree of hydration of VC was approximated from the evolution of compressive strength. Table 8 gives the obtained results.

For SCC, the drying depth was deduced for the four sealed curing durations, while for VC it was computed for $t_0 = 16$ h and $t_0 = 48$ h. The analysis clearly shows that the shorter sealed curing duration was the higher drying depth became, as shown in Fig. 15, Fig. 16 and Table 8. This is illustrated in Fig. 17.

The external layer of concrete specimens exposed to drying presents different microstructural characteristics from the concrete core. Longer

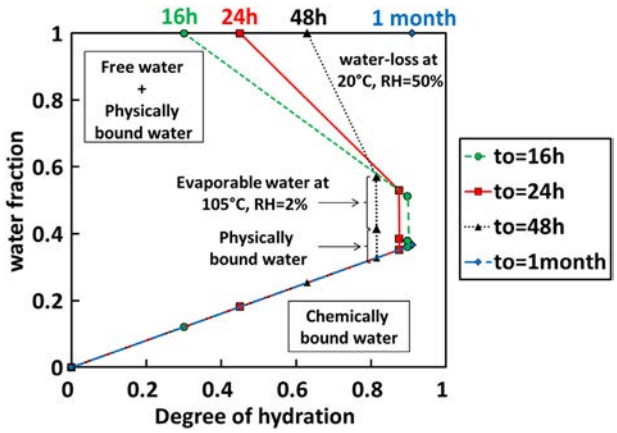

Fig. 10. Diagram of the volumetric phase distribution versus the degree of hydration for the four sealed curing durations for SCC.

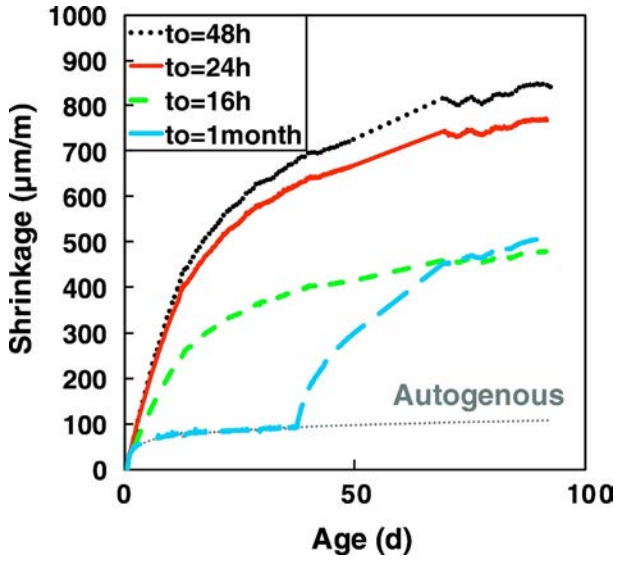

Fig. 11. Shrinkage vs. age for SCC.

sealed curing theoretically mitigates the extent of phenomena involved in drying depth. First, it reduces the coupling between hydration and drying. Long sealed curing duration actually allows better hydration of cement and makes concrete more homogeneous from surface to centre in terms of porosity. The drying depth actually decreased with the degree of hydration at t_0, when the specimens were exposed to drying (Fig. 18).

The first stage of drying shrinkage vs. mass loss curves, thus drying depth, has also been explained by microcracking induced by differential drying shrinkage [51,52]. The shrinkage of the external layer of concrete is actually restrained by the core of the specimen. Tensile stresses and microcracks are generated in the external layer, which is finally characterised by higher permeability [30]. Longer sealed curing allows better hydration thus surface concrete develops higher tensile strength, and it theoretically shows lower shrinkage induced cracking in the concrete skin.

According to the definition of this depth and for delayed formwork removal, the porous network becomes finer and the resistance to carbonation is improved. To verify these assumptions, the carbonation depth measurements and the results of porosimetry tests are discussed below.

Table 7
Ultimate drying shrinkage and shrinkage half time for different sealed curing periods.

		$t_0 = 16$ h	$t_0 = 24$ h	$t_0 = 48$ h	$t_0 = 1$ month
SCC	N_s (day)	15.7 ± 3	15.7 ± 2.4	14.9 ± 1.8	17.8
	ε_∞ (µm/m)	463 ± 17	841 ± 48	872 ± 6	545
VC	N_s (day)	13.9	14.1	4.5	x
	ε_∞ (µm/m)	446	711	788	x

3.2. Microstructure and carbonation

3.2.1. Carbonation

The results above could suggest that early formwork removal is the appropriate choice to reduce drying and total shrinkage. However, this first part of the study has not taken into account the durability issue. The phenomena leading to low drying shrinkage actually involve a relatively high carbonation risk. Previous studies actually stated that carbonated depth decreases with the curing duration [67 69].

The carbonated depths were measured at 6 months, 1 year or 4 years on concrete specimens exposed to drying at 20 °C, 50% RH, and 0.04% natural CO_2 concentration. Specimens exposed at $t_0 = 16$ h showed a 30% higher depth in comparison with $t_0 = 48$ h (Fig. 19 and Fig. 20). For $t_0 = 16$ h the carbonation increased by 6 mm between 6 months and 1 year, then between 1 year and 4 years. For $t_0 = 48$ h, this development seems to slow down over time. The specimen exposed at 1 month had a 4 year carbonated depth equivalent to 6 month depth of specimen exposed at $t_0 = 16$ h and that remained lower than the 1 year depths of all other specimens.

The progress of carbonation front is controlled by carbon dioxide diffusion that occurs through the concrete pores in gaseous phase. It depends on moisture, temperature, carbon dioxide concentration and concrete composition. The literature presents different empirical expressions to describe the carbon dioxide penetration. The function given by Tutti is based on the square root principle [70]. This mathematical function can also been found by resolving the differential equation of carbonation with simplifying assumptions [71]. To consider some

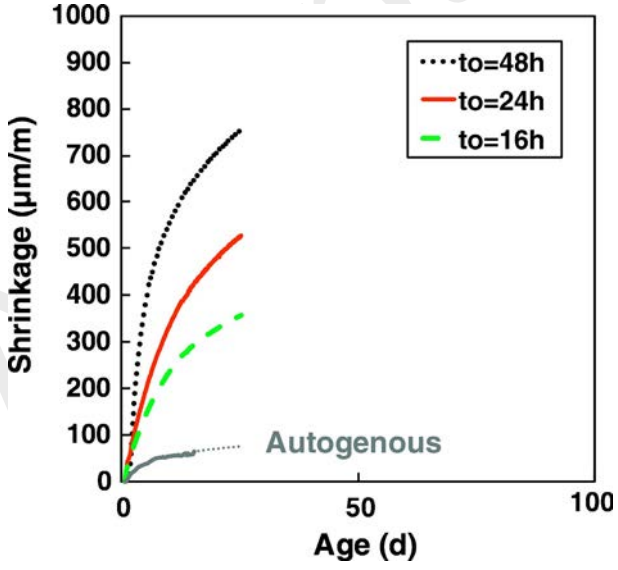

Fig. 12. Shrinkage vs. age for VC.

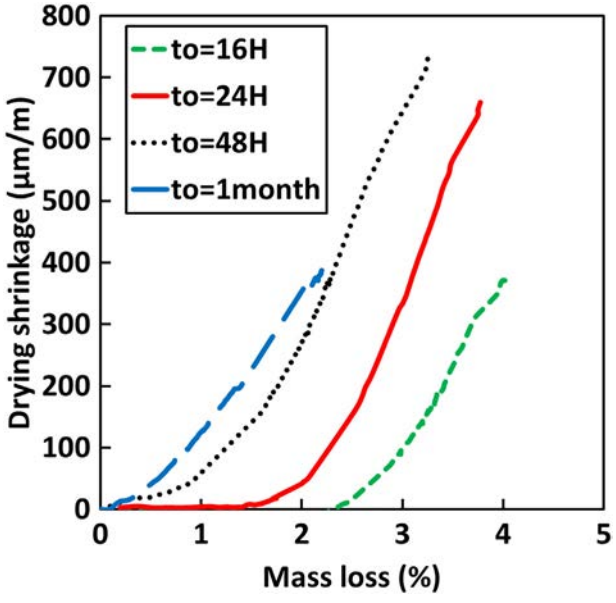

Fig. 13. Drying shrinkage vs. mass-loss for SCC.

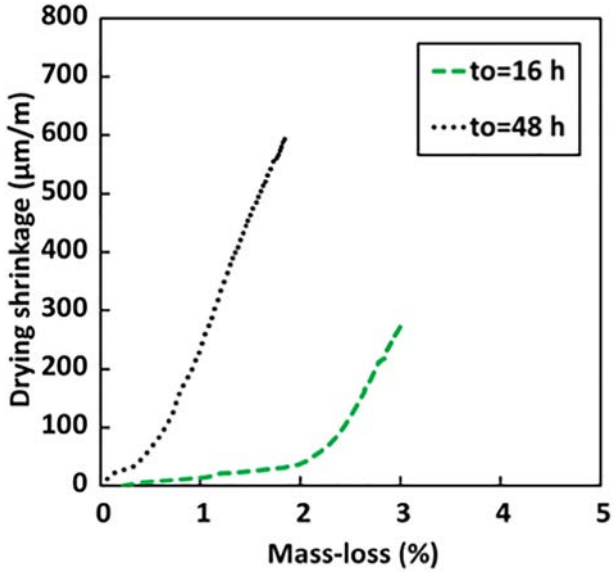

Fig. 14. Drying shrinkage vs. mass-loss for VC.

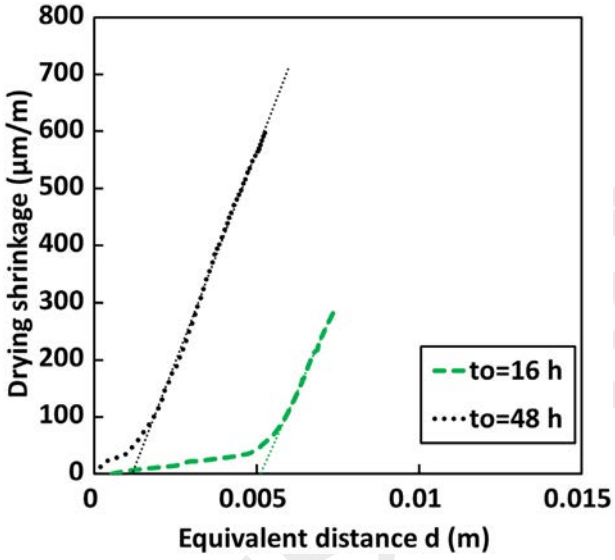

Fig. 16. Drying shrinkage vs. equivalent distance d of VC for two formwork durations.

factors affecting carbonation, several models based on Eq. (9) were developed using the same function [72].

$$x \quad k\sqrt{t} \tag{9}$$

where:

x is the carbonation depth (mm),
k is carbonation coefficient (mm/year$^{-1/2}$),
t is the time since exposure to CO_2 (year).

Based on this theory, a linear relation should be found when the carbonated depth is plotted as a function of the square root of time [73]. This was not the case in our experimental study, as shown in Fig. 21. The order of magnitude of carbonated depth at 6 months is the same as the drying depth. The diffusion of CO_2 is actually much faster in dry concrete than in saturated material [74]. The drying depth was also characterised by lower hydration degree. As shown by Xi et al. [77], the desorption isotherm depends on the hydration degree. For a given relative humidity, the shorter the curing time the lower the water saturation at equilibrium is. Concrete specimens exposed to drying and carbonation at $t_0 = 16$ h actually showed the highest carbonated depth after 6 month.

One of the assumptions leading to the square root function given in Eq. (9) is that concrete is a homogeneous material. This is not the case here as the diffusivity is higher in the drying depth and the degree of water saturation varies. When the carbonation front progresses inwards, the water saturation of concrete is higher and the diffusivity is lower, thus the carbonation coefficient decreases. The drying depth results showed an improvement of the homogeneity of concrete specimens with the sealed curing duration (Fig. 17). A microstructural analysis of the concrete layer could give clearer answers to this question.

Several studies showed a good statistical linear correlation between carbonated depth and compressive strength at time of exposure [69,75]. Since Fig. 7 showed a linear relation between strength and degree of hydration, a good linear correlation could be shown between carbonated depth and the degree of hydration at the time of exposure. Carbonated depth was plotted versus degree of hydration at t_0 in Fig. 21. At 6 months, 1 year or 4 years a good linear correlation has actually been found.

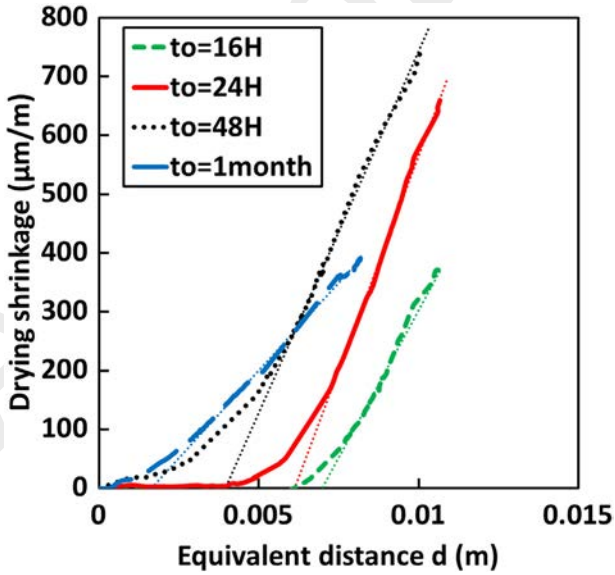

Fig. 15. Drying shrinkage vs. equivalent distance d of SCC for four formwork durations.

3.2.2. Porosimetry

Six months after casting, mercury intrusion porosimetry (MIP) was used to study the pore size distribution of the three sets of SCC specimens for ($t_0 = 16$ h, $t_0 = 24$ h and $t_0 = 48$ h). Cubic samples were picked from the middle and the edge of the cylinder. The cumulative porosity was plotted versus the pore diameter in Fig. 22 for $t_0 = 16$ h and Fig. 23 for $t_0 = 48$ h. Edge samples showed a significant decrease

Table 8
Drying depth for different sealed curing durations.

	t_0	16 h	24 h	48 h	1 month
SCC	α	0.30	0.45	0.63	0.91
	m_f (Kg/m^3)	180.3	167.9	153.0	129.9
	δ (mm)	7.0	6.1	4.0	1.7
VC	α[a]	0.14	0.30	0.48	0.87
	m_f (Kg/m^3)	171.4	159.3	145.6	116.1
	δ (mm)	5.1	x	1.2	x

[a] Degree of hydration estimated from compressive strength evolution [21].

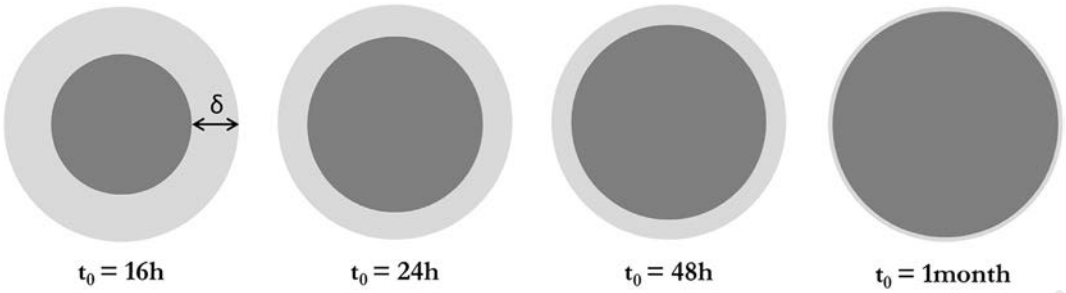

Fig. 17. The effect of the sealed curing duration on the drying depth.

of porosity from $t_0 = 16$ h to $t_0 = 48$ h. The effect of the sealed curing duration was much less pronounced on the specimen core. The difference between the edge and the centre was higher for reduced curing duration, which is consistent with the previous results given by the drying depth. The longer the sealed curing duration is the more uniform the pore sizes become.

The concrete samples used here contain various proportions of sand and gravel, for that reason, the average pore diameter can be misleading. The median pore diameter was chosen instead to analyse the MIP results. Its value actually decreased with the sealed curing duration in both series at the edge and the centre of specimens (Fig. 24). The median pore diameter was smaller in the centre where the hydration was less affected by drying.

The carbonation depth was plotted against the median pore diameter in Fig. 25 and a linearly increasing relationship was observed between these two parameters at the centre and the edge of specimens after 6 months, 1 year and 4 years.

Even if hydration, drying, and carbonation are very complex and coupled phenomena, this paper shows that simple linear correlation between five experimentally assessed parameters could be found. Compressive strength, degree of hydration at exposure, carbonated depth, median pore diameter, and drying depth were actually linked as summarized by Fig. 26. Thus, any of them can be used as a durability indicator.

3.3. Cracking

The durability of concrete exposed to carbonation was improved when the sealed curing duration increased. The porous network became finer and the carbonated depth decreased. Nevertheless, for drying shrinkage magnitude the existence of a pessimum for sealed curing duration for $t_0 = 48$ h or more was proven. Thus a clear conclusion cannot be drawn about durability before an estimation of the shrinkage induced cracking risk. The previously presented ring test was used to assess the cracking potential of SCC for three curing sealed durations: 16 h, 24 h and 48 h. To take into account the strain due to autogenous shrinkage the measurement started just after casting and it was carried on until cracking.

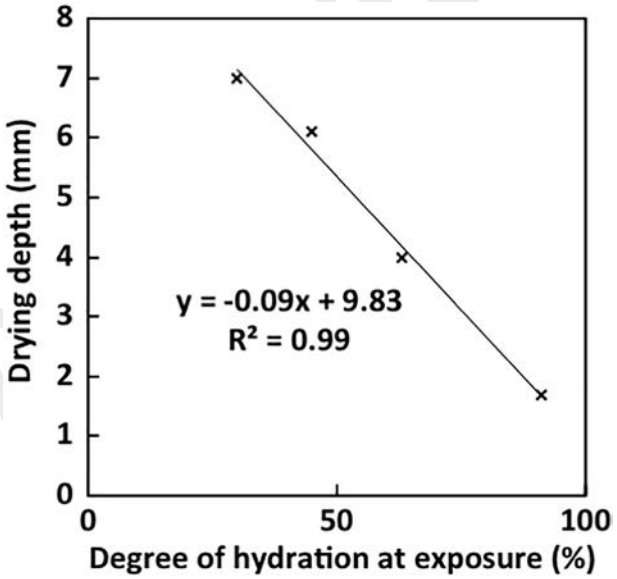

Fig. 18. Drying depth vs. degree of hydration at exposure for SCC.

Fig. 27 shows the time evolution of the tangential strain. Before demoulding, no significant difference was observed for the autogenous strain. Swelling was observed first. It was caused by thermal dilation due to hydration then followed by thermal contraction when the specimens were demoulded. The three curves were approximately the same. However, cracking occurs first for the specimen demoulded after 48 h, then for the one demoulded after 24 h. No cracking was observed for the ring cured for 16 h after 4 month monitoring. A lower drying shrinkage and stiffness were provided by the lower curing duration, which reduced cracking sensitivity of concrete. However the three curves were almost identical. This means that relaxation varied from one specimen to another. For $t_0 = 24$ h and $t_0 = 48$ h, the elastic stresses (free shrinkage × elastic modulus) were higher and the relaxation was not high enough to prevent concrete from cracking.

To assess the cracking risk for the three initial conditions tested here, the integrated criterion given by Eq. (3) was computed and given in Table 9. Based on a previous study [44], the estimated cracking risk went from low for $t_0 = 16$ h to medium for $t_0 = 24$ h and $t_0 = 48$ h. Thus the cracking risk of a given concrete mixture depends on the initial conditions, for instance the sealed curing duration.

3.4. Shrinkage model and discussion

Longer formwork duration allowed a development of the porous network towards a finer porous microstructure and a lower porosity. As far as shrinkage is concerned, this results in two conflicting evolutions, namely: an increase in negative fluid pressure and an increase in concrete elastic modulus.

According to the Young Laplace Eq. (10), and for a given water loss, finer pores lead to a higher fluid pressure due to capillary and disjoining pressures [76]. In this study the external RH was equal to 50%, which implies a higher internal RH in concrete specimens. For this range of RH in concrete, and for simplification in the first place the effect of surface forces can be neglected. From this point of view, it is consistent to obtain a higher drying shrinkage corresponding to the same water loss for specimens with a longer sealed curing duration.

$$\sigma_{cap} \quad \frac{2\sigma}{r}\, cos\alpha_m \tag{10}$$

σ: surface tension of gas liquid interface ($\sigma = 72.75.10^{-3}$ N·m^{-1} for water) [N·m^{-1}], r: pore radius [m], and α_m: wetting angle [rad].

The decrease in drying shrinkage from $t_0 = 48$ h to $t_0 = 1$ month could be partly explained by the increase of elastic modulus of concrete.

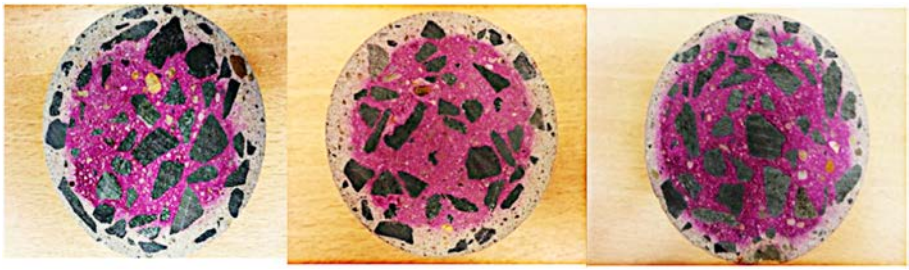

Fig. 19. Carbonated depths after 6 months of exposure, from left to right: $t_0 = 16$ h, $t_0 = 24$ h and $t_0 = 48$ h.

Young's modulus was actually 27% higher at 1 month (from 24.7 to 31.4 GPa, Table 3). This means that the strain generated by drying shrinkage for $t_0 = 1$ month would theoretically be 30% lower than for $t_0 = 48$ h. Moreover, considering the effect of creep, delayed loading in duces lower strains.

In order to understand the evolution of drying shrinkage magnitude and discuss possible mechanisms, a model has been written and the equations have been numerically solved. Based on the experimental col lected data, the drying shrinkage can be computed for different sealed curing durations. The first step consists in determining the evolution of the internal relative humidity for the cylindrical case. For that, the partial differential Eq. (11) must be solved:

$$\frac{\partial RH(r,t)}{\partial t} \quad \frac{1}{r}\frac{\partial}{\partial r}\left(\mathrm{D}\, r\, \frac{\partial \mathrm{RH(r,t)}}{\partial r}\right) \tag{11}$$

where D is the transport coefficient, and can be expressed as [77]:

$$\mathrm{D} \quad \alpha + \beta\left(1 - 2^{\ 10^{\gamma(RH\ \ 1)}}\right) \tag{12}$$

α,β and γ are calibrated coefficients which can be calculated from the concrete mixture proportions [77] ($\alpha = 0.0632$, $\beta = 1.0175$ and $\gamma = 9.3317$).

The initial condition is:

$$RH(r,0) \quad RH_i \tag{13}$$

and, the boundary conditions are:

$$RH(R,t) \quad RH_b \text{ and } \frac{\partial RH(0,t)}{\partial t} \quad 0 \tag{14}$$

for this study: $R = 3.9$ cm, $RH_b = 50\%$ and $RH_i = 100\%$.

From the solution of this non linear partial differential equation, the average RH along r can be assessed at each time step. This average value noted RH(t) will be used in the next stages of computations for simplification.

Then the capillary pressure can be deduced from relative humidity by [15]:

$$P_c(t) \quad -\frac{RT}{v_l^w}\left(\ln\left(\frac{RH(t)}{100}\right) + \ln\ 1 + \frac{n_l^{diss}}{n_l^w S(t)}\right)\right) \tag{15}$$

where

R is the universal gas constant (8.314 J·mol^{-1}·K^{-1}), and T is the temperature (293.15 K).

v_l^w is the molar volume of water ($1.82 \cdot 10^{-5}$ L·mol^{-1}).

n_l^{diss} is the concentration of dissolved species in the pore fluid (1.91 mol·L^{-1}).

n_l^w is the molar concentration of pure water (55 mol·L^{-1}).

The degree of saturation $S(t)$ can be deduced from the desorption isotherm. These curves can be computed from the mercury intrusion porosimetry (MIP) data by using the method described by Ranaivomanana [78]. The curves which correspond to the specimen

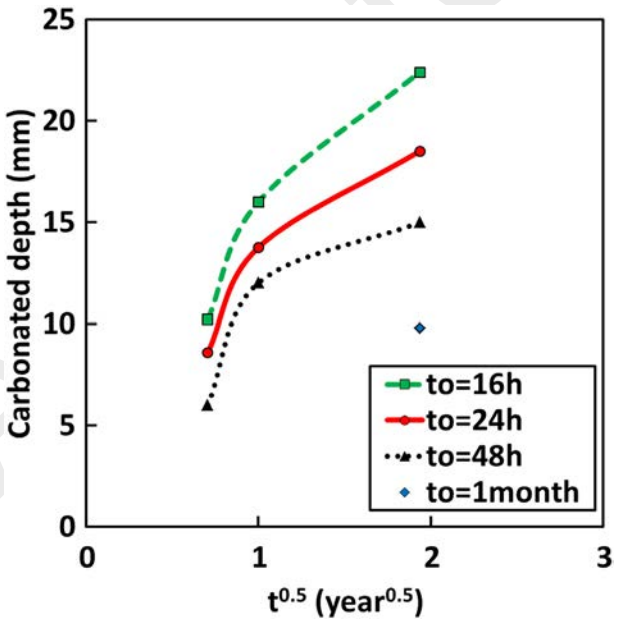

Fig. 20. Carbonated depth vs. square root of time for different sealed curing durations.

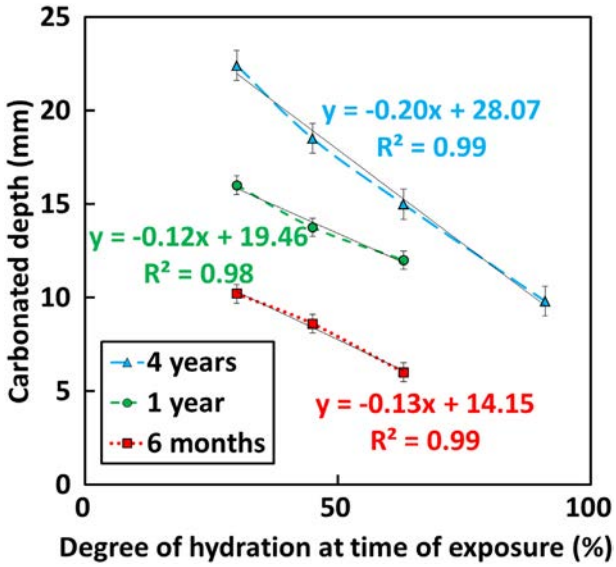

Fig. 21. Carbonated depth of SCC specimens vs. degree of hydration at time of exposure.

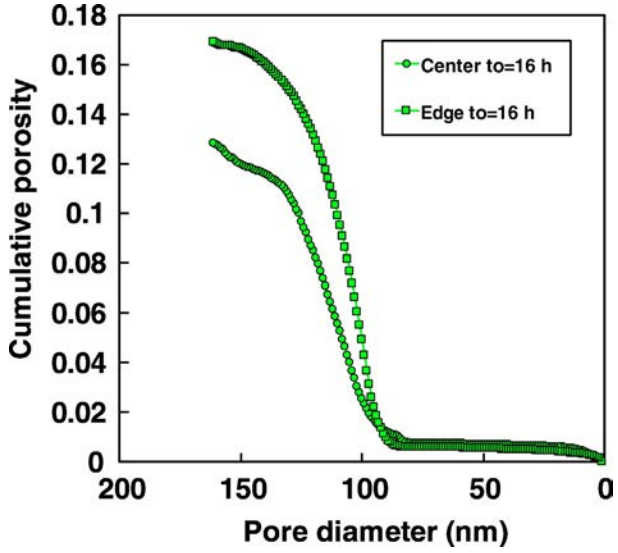

Fig. 22. Cumulative porosity vs. pore diameter for the centre and the edge of specimen for $t_0 = 16$ h.

centre were be considered for computation in this part. The rational mathematical form (Eq. (16)) has been chosen to fit the incomplete data provided by MIP and obtain the complete desorption curve.

$$S(t) \quad \frac{p_1 RH(t)^3 + p_2 RH(t)^2 + p_3 RH(t) + p_4}{RH(t)^2 + q_1 RH(t) + q_2} \tag{16}$$

p_i and q_i are fitting parameters. Despite the desorption isotherm curves depend on curing time [53], they were taken equal to the curves at the time of MIP tests. The curve for $t_0 = 1$ month has been deduced from the evolution of the parameters from $t_0 = 16$ h to $t_0 = 48$ h. The fitting parameters are gathered in the Table 10.

The pressure induced by interfaces can be described by [79]:

$$U \quad \int_S^1 P_c(S')\,dS' \tag{17}$$

and the effective pore pressure reads:

$$\xi \quad S P_c + U \tag{18}$$

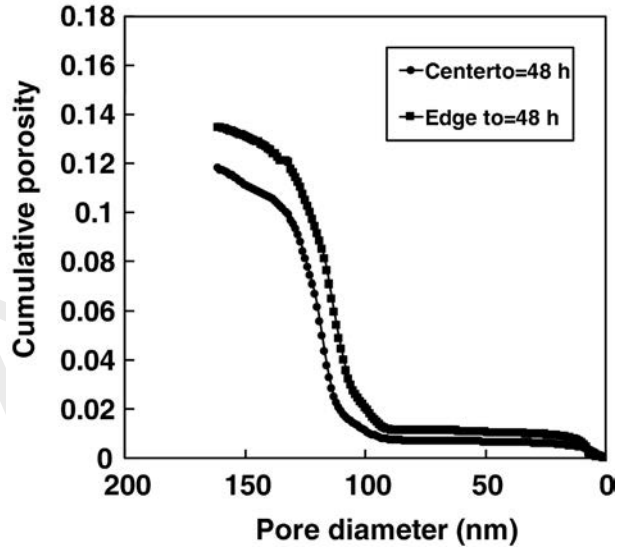

Fig. 23. Cumulative porosity vs. pore diameter for the centre and the edge of specimen for $t_0 = 48$ h.

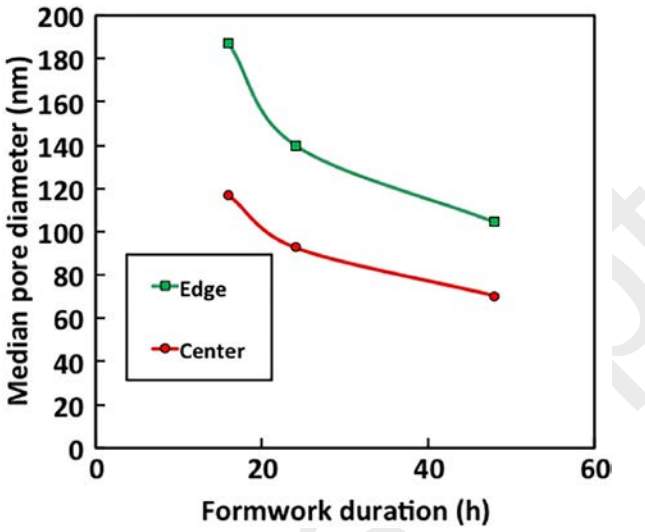

Fig. 24. Median pore diameter vs. formwork duration at the centre and the edge of specimen.

Finally, the axial free strain can be approximated by [80]:

$$\varepsilon(t) \quad \int_{t_0}^{t} \frac{\partial \xi(t')}{\partial t'} \left((1-2\vartheta) J(t-t_0) - \frac{1}{3K_s} \right) dt' \tag{19}$$

ϑ is the Poisson's ratio ($\vartheta = 0.2$), K_s is the bulk modulus for the solid phase ($K_s = 46$ GPa). $J(t - t_0)$ is the viscoelastic compliance and it can be expressed as:

$$\frac{1}{J(t-t_0)} \quad \left(p e^{-t/\tau} + (1-p) \right) E(t) \tag{20}$$

where p = 0.5 when $t_0 < 1$ month and p = 0.4 when $t_0 = 1$ month.

τ is the characteristic time and it is taken equal to 5 days.

E(t) is the evolution of Young's modulus deduced from experimental data using a fitting rational equation:

$$E(t) \quad \frac{at}{t+b} \tag{21}$$

where a and b are fitting parameters ($a = 38.29$ GPa and $b = 0.7652$ day).

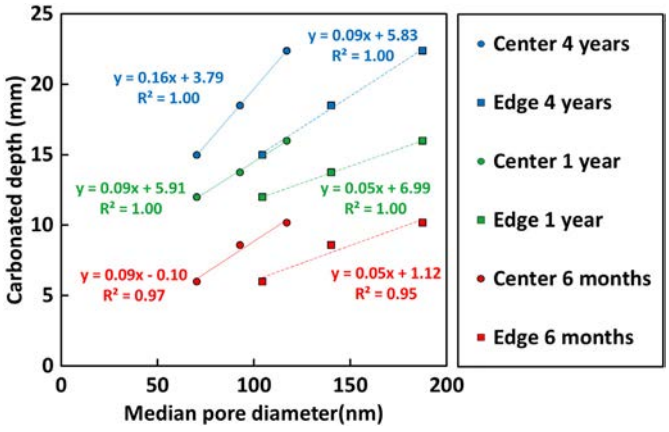

Fig. 25. Carbonated depth vs. median pore diameter at the centre and the edge of specimen after 6 months and 1 year.

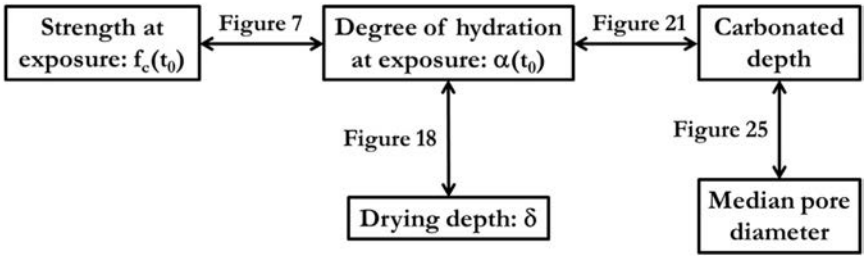

Fig. 26. Diagram of the linear relations between parameters.

The computed drying shrinkage for the four sealed curing durations is plotted in Fig. 28. Despite the calculated shrinkage magnitudes were different from the measured strains, the results confirm the pessimum effect. The highest developed strain was actually observed for $t_0 =$ 24 h then for $t_0 =$ 48 h, and the lowest for $t_0 =$ 16 h then for $t_0 =$ 1 month. These differences can be explained by some phenomena not accounted in our model such as: i) the temporal dependence of the de sorption isotherm, ii) the hydration influence on the degree of satura tion, the humidity and consequently on the effective pore pressure. iii) The actual evolution of the compliance under the effective pore pressure and internal relative humidity. iv) The influence of the specimen het erogeneity and the drying depth. Nevertheless, the aim of this simple model was not to reproduce the experimental values, which can be done for example by changing some input parameters, but to confirm that some assumptions on the mechanisms actually lead to a pessimum sealed curing duration for drying shrinkage. As a consequence, the rela tive drying shrinkage magnitude has been plotted against sealed curing duration in Fig. 29. Thereby, an area of maximum shrinkage can be ob served for the numerical and experimental results between $t_0 = 24$ h and $t_0 = 48$ h.

The observed pessimum sealed curing duration in the sense of shrinkage can be explained by the microstructure of the concrete when exposed to drying and specially two properties: the fineness of the porous network and the concrete elastic modulus. When drying time is delayed, the porous network becomes finer and for given water loss the corresponding internal stress increases. This stress gener ates a shrinkage strain, which depends on the concrete rigidity. The ul timate drying shrinkage actually increased for the three first sealed curing durations, then decreased for $t_0 = 1$ month despite higher inter nal stresses.

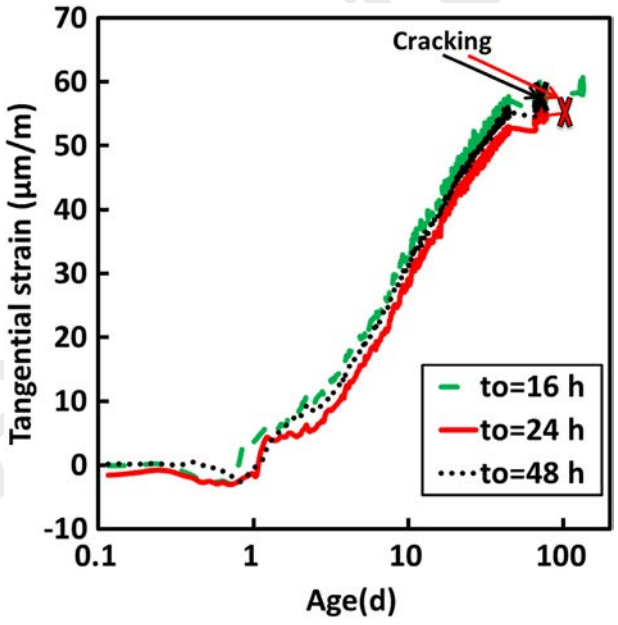

Fig. 27. Strain of the ring vs. age for SCC.

4. Conclusion

A comprehensive experimental study has been designed in order to investigate the influence of sealed curing duration on hydration, drying shrinkage induced cracking sensitivity, and resistance of concrete to natural carbonation. Two normal strength concretes have been studied, namely: self consolidating concrete and vibrated concrete. In this paper detailed results and quantitative information are given and correlated in order to deduce relatively simple rules governing these complex coupled phenomena.

- For a longer sealed curing duration, the hydration is more advanced when concrete is exposed to drying. Thus long term mass loss was lower due to weaker coupling between hydration and drying. Howev er, the reaction was less advanced for the long term. The amount of physically bound water was actually higher in this case and the free water available for hydration became relatively lower.
- The experimental evolution of drying shrinkage magnitude showed a maximum value between 24 and 48 hour sealed curing durations. A simple model and the numerical results confirmed some assumptions on the influence of mechanisms involved in drying shrinkage. The pessimum effect could be due to the competing effects of decreasing pore radii and increasing elastic modulus, as a function of sealed cur ing duration.
- This result can also be partly explained by the heterogeneity of drying concrete specimens. The drying depth, where the hydration degree is

Table 9
Integrated criterion for the three sealed curing durations.

SCC	16 h	24 h	48 h
Average strain rate factor: α ($10^{-6}/d^{0.5}$)	11.7	11.5	11.6
Elapsed time: t_{cr} (d)	>133	99	67
Stress rate: q (KPa/d)	94	107	131
Integrated criterion: $i_{cr} = S/t_{cr}$ (KPa/d^2)	<0.7	1.1	2.0

Table 10
Fitting parameters for the isotherm desorption curves.

Fitting parameters	$t_0 = 16$ h	$t_0 = 24$ h	$t_0 = 48$ h	$t_0 = 1$ month
p_1	0.7814	0.7436	0.7081	0.702
p_2	1.546	1.423	1.322	1.309
p_3	0.776	0.6833	0.6119	0.6042
p_4	0.001092	0.002538	0.008622	0.0095
q_1	2.246	1.994	1.945	1.945
q_2	1.258	0.9997	0.9519	0.9517

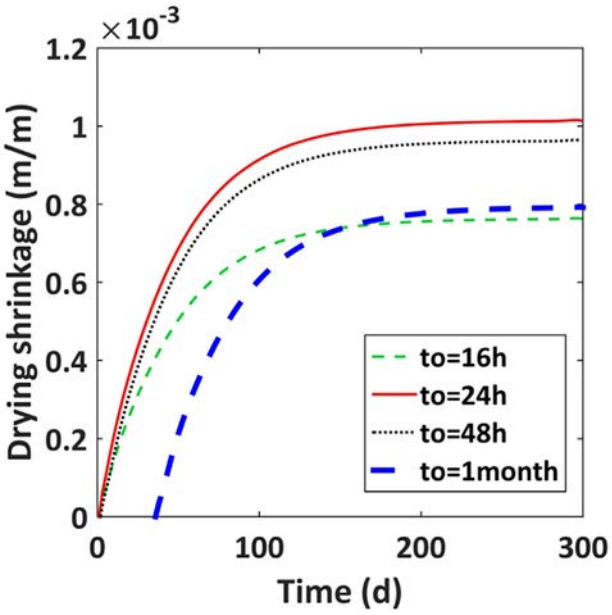

Fig. 28. Modeled drying shrinkage vs. time.

relatively low and free water is quickly lost, represents the area of the specimen that dries without generating shrinkage. The experimental results showed a linear decrease of the drying depth as a function of hydration degree at time of exposure to drying.

- The cracking risk increased with sealed curing duration, as shown by the integrated criterion deduced from restrained shrinkage tests. The SCC specimen with the shortest sealed curing did not crack. This could be related to lower shrinkage magnitude and lower elastic mod ulus, for equivalent strength. The influence of sealed curing duration on relaxation is still to be investigated.
- The longer the sealed curing the finer the porous network was. The concrete was more homogeneous with skin porosity closer to core po rosity. The resistance to carbonation was improved. Long term car bonated depth was actually found to depend on the degree of hydration at the time of exposure.
- In the range of studied parameters, linear correlation was shown be tween five properties: compressive strength and degree of hydration at exposure, carbonated depth, median pore diameter, and drying depth. Thereby, they could be used as durability indicators.

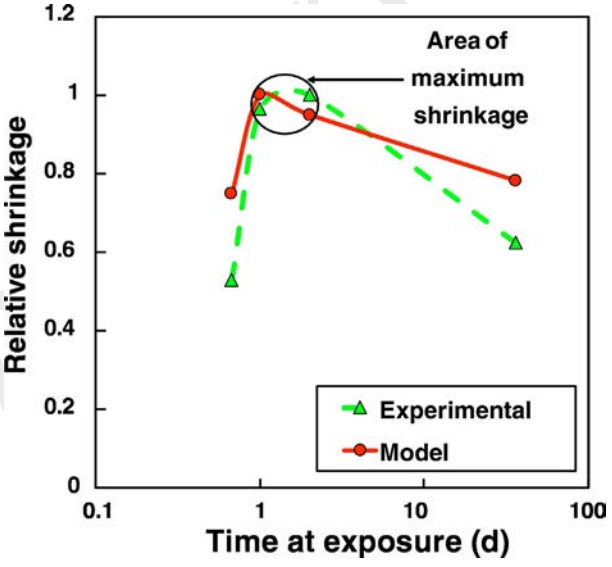

Fig. 29. Shrinkage relative to the maximum value vs. time at exposure.

Concrete is often defined by its composition, but this definition is not complete as the properties of concrete vary significantly as a function of other parameters, for instance sealed curing duration. Sealed curing should be as long as possible to allow hydration of cementitious mate rials and to ensure durability at long term. However, drying shrinkage shows a pessimum; this should be taken into account to avoid cracking of concrete cover to reinforcement.

Acknowledgements

The authors would like to thank French National Agency for Techno logical Research (ANRT), Edycem, and Bouygues Construction for their financial support and fruitful discussions.

References

[1] J.P. Balayssac, C.-H. Détriché, N. Diafat, Influence de la durée d'une cure humide sur les caractéristiques mécaniques de bétons d'usage courant (Effect of wet curing duration upon mechanical properties of commonly-used concretes), Mater. Struct. 30 (June) (1997) 284–292.
[2] S.H. Al-Ani, M.A.K. Al-Zaiwary, The effect of curing period and curing delay on concrete in hot weather, Mater. Struct. 21 (1988) 205–212.
[3] I. Soroka, A. Bentur, H. Jaegermann, Short-term steam-curing and concrete later-age strength, Mater. Struct. 11 (2) (1978) 93–96.
[4] Cahier des clauses techniques générales applicables aux marchés publics de travaux. Fascicule N°65. Exécution des ouvrages de génie civil en béton armé ou précontraint, 2012.
[5] Q. City, T. Adam, O. Kroggel, P. Gruebl, Influence of the relative humidity on the hydration kinetics of concrete, 2nd International Symposium on Advances in Concrete through Science and Engineering September 2006, pp. 11–13 (Quebec City, Canada, 2006, no. September).
[6] J. Monge, Fissuration des mortiers en couches minces - Effet de l'hydratation, du séchage et de la carbonatation(In french) PhD, ENS Cachan, 2007.
[7] J. Monge, Caractérisation et modélisation de l'effet du séchage sur la fissuration d'une couche mince de mortier, XXVèmes Rencontres Universitaires de Génie Civil 2007, pp. 1–8 (In french).
[8] T. Mauroux, Impact du séchage sur les propriétés d'adhérence entre un mortier et un support: influence de l'adjuvantation par des éthers cellulose(In french) PhD, Université de La Rochelle, 2011.
[9] H. Samouh, E. Rozière, A. Loukili, Influence of formwork duration on shrinkage, microstructure, and durability of cement based materials, ConCreep, 2015.
[10] A. Alhozaimy, P. Soroushian, F. Mirza, Effects of curing conditions and age on chloride permeability of fly ash mortar, ACI Mater. J. 93 (1) (1996) 87–95.
[11] S. Miyazawa, E. Tazawa, Influence of specimen size and relative humidity on shrinkage of high-strength concrete, Concr. Sci. Eng. 3 (March) (2001) 39–46.
[12] T. Aly, J.G. Sanjayan, Mechanism of early age shrinkage of concretes, Mater. Struct. 42 (4) (May 2008) 461–468.
[13] A. Hajibabaee, M.T. Ley, The impact of wet curing on curling in concrete caused by drying shrinkage, Mater. Struct. 49 (5) (2016) 1629–1639.
[14] A. Hajibabaee, M.T. Ley, Impact of wet and sealed curing on curling in cement paste beams from drying shrinkage, ACI Mater. J. 112 (1) (2015) 79–84.
[15] A. Hajibabaee, Z. Grasley, M.T. Ley, Mechanisms of dimensional instability caused by differential drying in wet cured cement paste, Cem. Concr. Res. 79 (2016) 151–158.
[16] W. Perenchio, The drying shrinkage dilemma, Concr. Constr. 42 (1997) 379–383.
[17] K. Kovler, O.M. Jensen, RILEM Technical Committee 196-ICC, Internal Curing of Concrete, 2007.
[18] M. Bouasker, P. Mounanga, P. Turcry, A. Loukili, A. Khelidj, Chemical shrinkage of cement pastes and mortars at very early age: effect of limestone filler and granular inclusions, Cem. Concr. Compos. 30 (1) (Jan. 2008) 13–22.
[19] A.F. Stock, D.J. Hannant, R.I.T. Williams, The effect of aggregate concentration upon the strength and modulus of elasticity of concrete, Mag. Concr. Res. 31 (109) (1979) 225–234.
[20] M. Neville Adam, Concrete Properties, Fifth Edit, Trans-Atlantic Publications, 2012.
[21] K. van Breugel, Simulation of Hydration and Formation of Structure in Hardening Cement-based Materials, Technical University Delft, 1991.
[22] T. Lenormand, E. Rozière, A. Loukili, S. Staquet, Incorporation of treated municipal solid waste incineration electrostatic precipitator fly ash as partial replacement of Portland cement: effect on early age behaviour and mechanical properties, Constr. Build. Mater. 96 (2015) 256–269.
[23] S. Medjigbodo, A. Darquennes, C. Aubernon, A. Khelidj, A. Loukili, Effects of the air-steam mixture on the permeability of damaged concrete, Cem. Concr. Res. 54 (2013) 98–105.
[24] T.C. Hansen, Physical structure of hardened cement paste. A classical approach, Mater. Struct. 19 (6) (1986) 423–436.
[25] A. Loukili, A. Khelidj, P. Richard, Hydration kinetics, change of relative humidity, and autogenous shrinkage of ultra-high-strength concrete, Cem. Concr. Res. 29 (4) (Apr. 1999) 577–584.

[26] Z.P. Bazant, S. Baweja, RILEM technical committees 107-GCS guidelines for the formulation of creep and shrinkage prediction models, Mater. Struct. 107 (1995) 415–430.
[27] H. Samouh, Nouvelles approches des relations entre formulation et comportement différé des matériaux cimentaires: application aux bétons autoplaçants(In french) PhD, Ecole Centrale de Nantes, 2015.
[28] Z.C. Grasley, D.A. Lange, M.D. D'ambrosia, S. Villalobos-chapa, Relative humidity in concrete, ACI Comm. 236 (October) (2006) 51–57.
[29] V. Baroghel-bouny, J. Godin, Experimental study on drying shrinkage of ordinary and high-performance cementitious materials, RILEM Conf. Shrinkage 3 (9) (2001) 13–22.
[30] H. Samouh, A. Soive, E. Rozière, A. Loukili, Experimental and numercial study of size effect on long-term drying behavior of self-consolidating concrete: influence of drying depth, Mater. Struct. 49 (10) (2016) 4029–4048.
[31] H. Samouh, E. Rozière, A. Loukili, Interprétation des mesures du retrait de dessiccation des bétons autoplaçants (BAP), XXXe Rencontres AUGC-IBPSA. Chambéry,Savoie, 6au 8 Juin 2012, 2012 (In french).
[32] European standard, Eurocode 2: Design of Concrete Structures EN1992-1-1, 2004 1–250.
[33] ACI Committee 209, Guide for Modeling and Calculating Shrinkage and Creep in Hardened Concrete, 2008.
[34] T.C. Hansen, A.H. Mattock, Influence of size and shape of member on the shrinkage and creep of concrete, J. Am. Concr. Inst. 63–10 (1966) 267–290.
[35] P.J. Dees, J. Polderman, Mercury porosimetry in pharmaceutical technology, Powder Technol. 29 (1) (May 1981) 187–197.
[36] E. Rozière, A. Loukili, F. Cussigh, A performance based approach for durability of concrete exposed to carbonation, Constr. Build. Mater. 23 (1) (Jan. 2009) 190–199.
[37] A. Younsi, P. Turcry, E. Rozire, A. Ait-Mokhtar, A. Loukili, Performance-based design and carbonation of concrete with high fly ash content, Cem. Concr. Compos. 33 (10) (2011) 993–1000.
[38] ASTM C1581-04: Standard Test Method for Determining Age at Cracking and Induced Tensile Stress Characteristics of Mortar and Concrete Under Restrained Shrinkage, 2004.
[39] K. Kovler, A. Bentur, Cracking sensitivity of normal- and high-strength concretes, ACI Mater. J. (106) (2009) 537–542.
[40] S. Zhutovsky, K. Kovler, A. Bentur, Effect of hybrid curing on cracking potential of high-performance concrete, Cem. Concr. Res. 54 (Dec. 2013) 36–42.
[41] AASHTO PP34-99: Standard Practice for Cracking Tendency Using a Ring Specimen, 2005.
[42] J.-H. Moon, F. Rajabipour, B. Pease, J. Weiss, Quantifying the influence of specimen geometry on the results of the restrained ring test, J. ASTM Int. 3 (8) (2006) 1–14.
[43] P. Turcry, A. Loukili, K. Haidar, G. Pijaudier-cabot, A. Belarbi, Cracking tendency of self-compacting concrete subjected to restrained shrinkage: experimental study and modeling, J. Mater. Civ. Eng. (2006).
[44] H. Samouh, Evaluation de la sensibilité à la fissuration des BAP: Apport de l'analyse du comportement viscoélastique, Prix jeune chercheurs “René Houpert”. ISABTP/UPPA, Anglet, 27 au 29 Mai 2015, 2015 (In french).
[45] H. Samouh, E. Roziere, A. Loukili, Self-consolidating concrete cracking sensitivity: cracking index and database, SCC 2016 8th International RILEM Symposium on Self-compacting Concrete: Flowing toward Sustainability 2016, pp. 709–719.
[46] J. Torrenti, La résistance du béton au très jeune âge, Bull. Liaison des Lab. des Ponts Chaussées 179 (April) (1992) 31–41.
[47] I. Odler, M. Yudenfreund, J. Skalny, S. Brunauer, Hardened portland cement pastes of low porosity III. Degree of hydration. Expansion of paste. Total porosity, Cem. Concr. Res. 2 (4) (1972) 463–480.
[48] I. Odler, H. Dorr, Early hydration of tricalcium silicate I. Kinetics of the hydration process and the stoichiometry of the hydration products, Cem. Concr. Res. 9 (2) (1979) 239–248.
[49] F.S. Rostasy, M. Laube, Experimental and analytical planning tools to minimize thermal cracking of young concrete, Testing During Concrete Construction: Proceedings of an International RILEM Workshop 1990, pp. 207–223.
[50] G. De Schutter, L. Taerwe, Degree of hydration-based description of mechanical properties of early age concrete, Mater. Struct. 29 (July) (1996) 335–344.
[51] B. Bissonnette, P. Pierre, M. Pigeon, Influence of key parameters on drying shrinkage of cementitious materials, Cem. Concr. Res. 29 (July) (1999) 1655–1662.
[52] O.M. Jensen, P.F. Hansen, Water-entrained Cement-based Materials I. Principles and Theoretical backgrOund, vol. 31, 2001 647–654.
[53] Y. Xi, Z.P. Bazant, H.M. Jennings, Moisture diffusion in cementitious materials. Adsorption isotherms, Adv. Cem. Based Mater. (1994) 248–257.
[54] H.S. Müller, C.H. Küttner, V. Kvitsel, Creep and shrinkage of normal and high performance concrete – concept for a unified code-type approach, Rev. Française Génie Civ. 3 (3–4) (1999) 113–132.
[55] E. Rozière, S. Granger, P. Turcry, A. Loukili, Influence of paste volume on shrinkage cracking and fracture properties of self-compacting concrete, Cem. Concr. Compos. 29 (8) (Sep. 2007) 626–636.
[56] E. Rozière, A. Khelidj, Chapter 4: durability of self-compacting concrete, in: A. Loukili (Ed.), Self Compacting Concrete, ISTE, Wiley, 2011.
[57] T. Mauroux, F. Benboudjema, P. Turcry, A. Ait-Mokhtar, O. Deves, Study of cracking due to drying in coating mortars by digital image correlation, Cem. Concr. Res. 42 (7) (2012) 1014–1023.
[58] fib Model Code for Concrete Structures 2010, 2013.
[59] ACI Committee 209, Guide for Modeling and Calculating Shrinkage and Creep, 2008.
[60] R. Wendner, M.H. Hubler, Z.P. Bazant, The B4 model for multi-decade creep and shrinkage prediction, Proceedings of the Ninth International Conference on Creep, Shrinkage, and Durability Mechanics (Concreep-9) 2013, pp. 429–436.
[61] M.D. Nguyen, M. Thiery, P. Belin, A model for hydration-drying interactions in the concrete cover, Thermo-Hydromechanical and Chemical Coupling in Geomaterials and Applications: Proceedings of the Third International Symposium GeoProc 2008, pp. 553–562.
[62] F. Benboudjema, F. Meftah, J.M. Torrenti, Interaction between drying, shrinkage, creep and cracking phenomena in concrete, Eng. Struct. 27 (2) (Jan. 2005) 239–250.
[63] C. de Sa, F. Benboudjema, M. Thiery, J. Sicard, Analysis of microcracking induced by differential drying shrinkage, Cem. Concr. Compos. 30 (10) (Nov. 2008) 947–956.
[64] P.C. Kreijger, The skin of concrete composition and properties, Mater. Constr. 17 (1972) 275–283.
[65] C. Andrade, J.M. Diez, C. Alonso, Mathematical modeling of a concrete surface ' skin effect ' on diffusion in chloride contaminated media, Adv. Cem. Based Mater. 6 (2) (1997) 39–44.
[66] H. Samouh, E. Rozière, A. Loukili, Drying depth and size effect on long-term behavior of concrete, Key Eng. Mater. 711 (2016) 645–651.
[67] J.P. Balayssac, C.H. Détriché, J. Grandet, Effects of curing upon carbonation of concrete, Constr. Build. Mater. 9 (2) (1995) 91–95.
[68] F. Pacheco Torgal, S. Miraldo, J.A. Labrincha, J. De Brito, An overview on concrete carbonation in the context of eco-efficient construction: evaluation, use of SCMs and/or RAC, Constr. Build. Mater. 36 (2012) 141–150.
[69] C.D. Atis, Accelerated carbonation and testing of concrete made with fly ash, Constr. Build. Mater. 17 (3) (2003) 147–152.
[70] K. Tuutti, Corrosion of Steel in Concrete, 1982.
[71] V.G. Papadakis, C.G. Vayenas, M.N. Fardis, Fundamental modeling and experimental investigation of concrete carbonation, ACI Mater. J. 88 (4) (1991) 363–373.
[72] I. Monteiro, F.A. Branco, J. De Brito, R. Neves, Statistical analysis of the carbonation coefficient in open air concrete structures, Constr. Build. Mater. 29 (2012) 263–269.
[73] F. Buyle-Bodin, R. Hadjieva-Zaharieva, Influence of industrially produced recycled aggregates on flow properties of concrete, Mater. Struct. 35 (October) (2002) 504–509.
[74] V. Papadakis, C. Vayenas, M. Fardis, Physical and chemical characteristics affecting the durability of concrete, ACI Mater. J. 8 (88) (1991) 186–196.
[75] H. Zhao, W. Sun, X. Wu, B. Gao, Effect of initial water-curing period and curing condition on the properties of self-compacting concrete, Mater. Des. 35 (2012) 194–200.
[76] T.C. Powers, The thermodynamics of volume change and creep, Mater. Struct. 1 (6) (1968) 487–507.
[77] Y. Xi, Z.P. Bazant, L. Molina, H.M. Jennings, Moisture diffusion in cementitious materials. Moisture capacity and diffusivity, Adv. Cem. Based Mater. (1994) 258–266.
[78] H. Ranaivomanana, J. Verdier, A. Sellier, X. Bourbon, Toward a better comprehension and modeling of hysteresis cycles in the water sorption–desorption process for cement based materials, Cem. Concr. Res. 41 (8) (Aug. 2011) 817–827.
[79] O. Coussy, P. Dangla, T. Lassabatere, V. Baroghel-Bouny, The equivalent pore pressure and the swelling and shrinkage of cement-based materials, Mater. Struct. 37 (January–February) (2004) 15–20.
[80] Z.C. Grasley, C.K. Leung, Desiccation shrinkage of cementitious materials as an aging, poroviscoelastic response, Cem. Concr. Res. 41 (1) (Jan. 2011) 77–89.